# An Illustration Technique for Unstructured 3-D Meshes *

N P Konrad and R B Simpson
University of Waterloo
Department of Computer Science
Technical Report CS-93-30

November 1, 1993

**Abstract**

Geometric relations in an irregular 3-D polyhedron or tetrahedral mesh are often difficult to comprehend, even for relatively few vertices. A technique for illustrating such meshes which aids this comprehension is described in terms of several independent components, i.e. edge representation, viewpoint and perspective projection, and lighting. These images are suitable for embedding in dynamic displays, or in publications. Heuristics for the effective use of these components are discussed and the technique is demonstrated on three small configurations from the recent literature.

## 1 Introduction

A general configuration in three dimensions of vertices and edges will be referred to as a 3-D unstructured mesh. Examples are polyhedra or the general tetrahedral meshes of computer-aided design or the finite element method. They differ from general graphs because the locations of the vertices in space are fixed, a priori. For 3-D meshes with even relatively few vertices, it can be difficult to comprehend the incidence relations between the geometric objects in the mesh, or sketch useful diagrams freehand. In this paper, we discuss a technique for creating images of small 3-D unstructured meshes to aid their comprehension. We present the several components of the construction of these images as a single technique to make a coherent, brief presentation; however, these components are largely independent and many variations are possible.

We are particularly interested in the application of this technique to submeshes of tetrahedral meshes. These special unstructured 3-D meshes are fundamental discretizations of three space, and are currently under active study in computational geometry, computer aid geometry, computer aided design and the finite element method. Their use can be expected to increase as lower cost/performance ratios for workstations broaden participation in 3-D

*Support for this research was provided by the Natural Sciences and Engineering Research Council of Canada, and by the Information Technology research Centre of Ontario. Helpful discussions with W B Cowan are gratefully acknowledged.

modeling. This is a quite specific application which can be served by the relatively simple graphics techniques we discuss, but it is a significant one which is not being well addressed in current practices. A look at papers from any of the above mentioned applications areas shows that a standard practice continues to be the representation of edges by differing line types, solid, dashed, dots, variable widths (see, e.g., the original figures for the examples of §4). We note an early exception in [Wat81] where stereoscopic images were presented , and [Moo92] in which a technique has been used based on exploding solid components of a decomposition , plus directional lighting; but exceptions are truly exceptional.

Typical identification tasks for which these illustrations should provide clarification would be:

- For a given edge (or face), identify the tetrahedra incident on it.
- For a given tetrahedron, identify its neighbours in the mesh.

Examples appearing in recent literature are used in §4 to demonstrate how the technique supports these tasks. Normally, one does not rely solely on a single image to understand a mesh. The image may be part of a dynamic graphical display, in which case, motion, or interactive manipulation of the image are strong aids to comprehension. In publications, the combination of image and supporting text jointly direct the process of understanding, as we indicate in the demonstrations section of this paper.

Displaying an unstructured mesh is a more constrained image creation task than the more commonly studied problem of displaying a 3-D representation of a general graph (e.g. [C+92] and bibliography). We also distinguish the goals of this technique from those of illustrations of large segments of finite element meshes, which typically show hundreds of triangular faces in a planar cut through a 3-D mesh. These latter illustrations are useful for conveying general impressions, for example of vertex distributions, but do not support the detailed identification tasks referred to above.

In the next section, we describe the components of the technique and make some observations about their connections to the psychology of perception. These components are typically available in commercial packages supporting 3-D graphics which should make the technique broadly accessible. In the following section, §3, we discuss some heuristics of using these components to form mesh images, to serve our comprehension goals.

## 2 Components of the Illustration Technique

Figure 1 shows an illustration of a decomposition of a prism. We invite the reader to observe that the interior edge $gh$ has three tetrahedra incident on it, none of which have faces on the boundary of the prism.

The illustration components of the technique exemplified in this figure are:

- the representation of edges
- the viewpoint and perspective
- the lighting

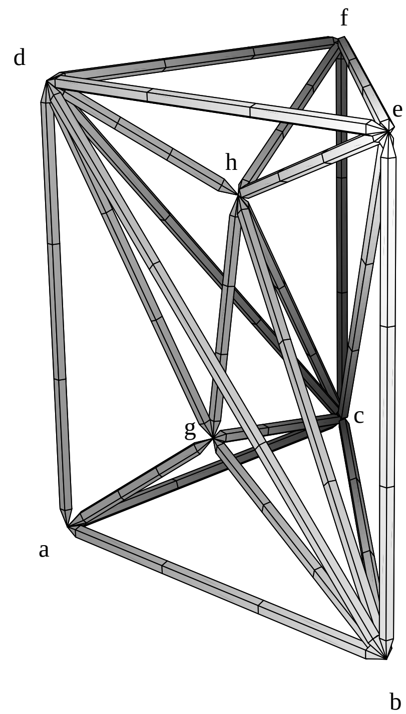


Figure 1: Decomposition of a prism

The edges in Figure 1 are projected images of five sided tubes in space, with bevelled ends, which we will refer to as edge beams. Each tube consists of five panels, which are long thin rectangles. Each bevel is a triangular face joining the narrow end of a beam panel to the end vertex of the edge being represented. For a particular choice of viewing position, the panels and bevels of the edge beams are rendered with Gouraud shading based on diffuse light originating from the viewing point. A painter's algorithm is used to render the projections of these polygons blending their grey scales over the interior of each and superimposing them. The success of this approach depends on the ability of the painter's algorithm to correctly order the projected polygons. For example, if 3-D graphics software is used which orders polygons according to the depth coordinate of their centroid, then it may misrepresent the ordering of long beam panels that overlap near one end. To rectify this, it may be more reliable (at increased computation) to represent a beam panel by a series of rectangles of less extreme aspect ratio. A comparable use of single panels to represent arcs in graph displays in a virtual reality context is reported in [WHF93].

Choosing a viewing position involves selecting viewing angles, elevation and azimuth, as well as a viewing distance from the centre of the object. We adopt a standard viewing distance, in which the diameter of the projected image subtends an angle of 25 degrees at the viewing point, which we will refer to as the standard viewing perspective. A suitable choice of viewing angles must be customized for each configuration as discussed below.

**Connections to the psychology of perception**

We cannot expect to 'prove' the effectiveness of these components through recourse to the classical theory of perception. However, we can perhaps gain some confidence from the

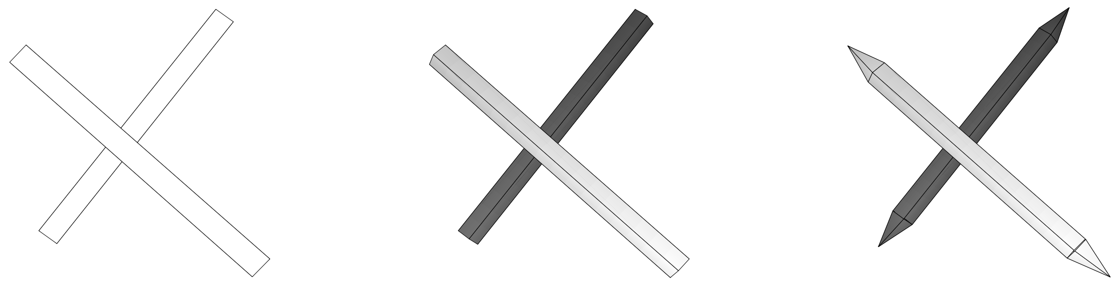

a b c

Figure 2: Perception phenomena of continuation and interposition

extent to which they seem related to phenomena known to enhance recognition of three dimensional objects from planar images. Some of these phenomena have been of interest to artificial intelligence research in computer vision and are reviewed in the special issue [Bob81]. A 10 year retrospective on some of this work is provided in [BT93], and a useful reference on the psychology of perception is [Roc75].

Our choice of edge beams to represent edges is strongly connected to two related perception phenomena, continuation and interposition, whereby the 6 line segments of Figure 2a are commonly perceived as two overlapping strips. The effect of a pattern between the pairs of line segments is to enhance the continuity effect as indicated in Figure 2b. We note that the effect of edge panel lighting, while intended to enhance depth perception, does not detract from this effect. It is well known that the treatment of line endings plays an important role on the perception of form in an image. The use of end bevels to complete edge beams enhances their image as a spatial object as indicated in Figure 2c; it is simple to implement, and identifies the location of the vertices.

Certain configurations of lines evoke a a strong tendency to interpret them as the outline of a three dimensional object. An example used commonly to illustrate this is shown in Figures 3 and 4 (more typically displayed with simple lines for edges). Although there is an infinity of three dimensional structures that have this projected image, this figure is interpreted as a cube almost universally. A common psychological explanation for this phenomenon is based on the hypothesis that our perception mechanism actively seeks to interpret a 2-D image as either a 2-D object or the projection of a 3-D object automatically. Of all the possible interpretations, this mechanism selects one that is most likely, or most natural , or simplest; a criterion sometimes referred to as the principle of simplicity. This hypothesis provides an explanation for the familiar phenomenon of reversal for Figure 4a, discussed in the next section, as arising because two interpretations are deemed equally simple. The psychology of the simplicity criterion continues to be a research topic.

In view of this, an important strategy for producing illustrations that enhance comprehension of unstructured meshes is to seek an image for which this phenomenon supports the desired interpretation. Our experience has been that this depends critically and sensitively on the viewpoint taken in the image creating projection. Unfortunately, sometimes the goal

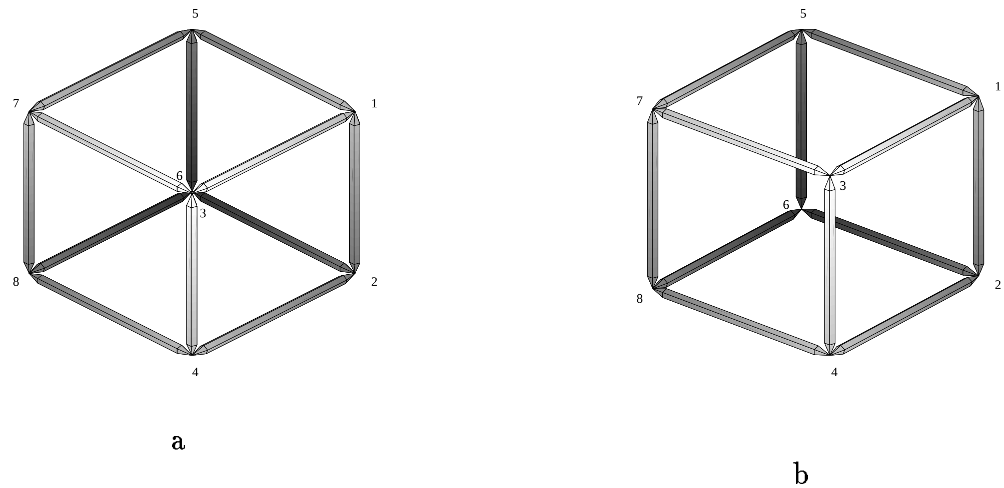


Figure 3: The projection of a cube - 1

of the illustration is to provide an example that is counter intuitive or at least unfamiliar, in which case the illustration strategy must work against this phenomenon. We provide a small example in the second demonstration of §4.

We have experimented with a number of variations of these (and other) components, but present here a single choice which seems to be a good balance of effectiveness and simplicity. This latter is a consideration because we would like a technique which can be used in general publication practice, and which can be readily realizable by authors with access to basic 3-D graphics software. The technique can, of course, be embedded in dynamic displays, and enhanced with colour, to provide a more powerful on-line tool. In another extension of this basic technique, specific features in a mesh could be given special treatment to illustrate some point; however, we present the technique as illustrating meshes homogeneously.

# 3 Heuristics

In this section, we discuss some heuristic observations based on our experimenting with the techniques just described. It seems clear that the use of edge beams, and the location of the viewpoint are the primary mechanisms for enhancing the interpretation of illustrations of meshes. The choice of perspective and lighting seem to be secondary effects. The familiar projection of a cube will be used to demonstrate the role of viewpoint and edge beams in this illustration technique. We will then discuss heuristics of the primary mechanisms in more detail.

In Figure 3a, the viewpoint is selected so that the images of the cube vertices 3 and 6 coincide. In Figure 3b both azimuth and elevation have been decreased by five degrees. In both cases, the standard edge beams and lighting have been used, with an orthographic projection. The interpretation of Figure 3b as a cube seen from above with vertex 3 in the foreground is apparent, and is a commonly used example of the 'simplicity' principle of

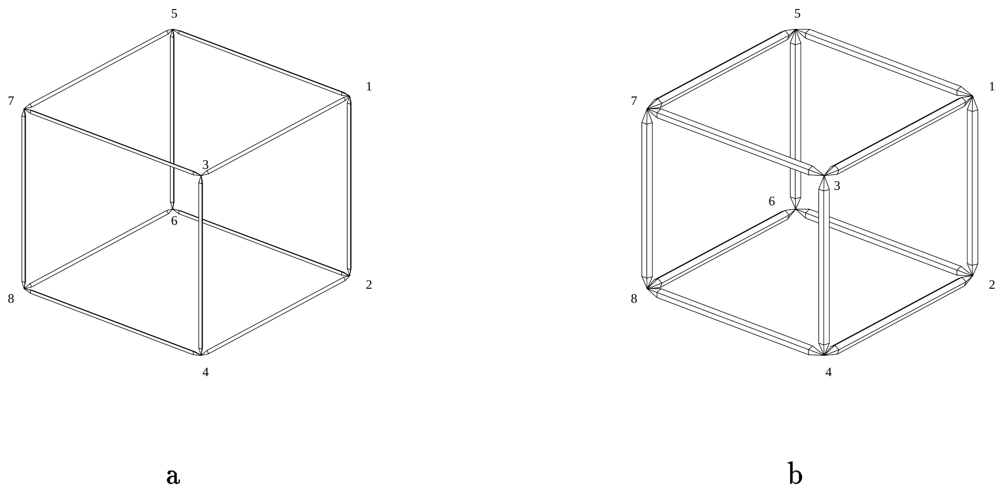


Figure 4: The projection of a cube - 2

interpreting 2-D images discussed in §2. For Figure 3a, an interpretation that is at least equally plausible is that it represents a 2-D hexagon comprised of 6 equilateral triangles. The viewpoint of this latter figure has obviously reduced the contribution of the edge beams to the 3-D interpretation and the gray scale shading is relatively ineffective in contributing to this latter interpretation. The effect of using the standard perspective in these figures is essentially the same.

If the image of the cube as shown from the viewpoint of Figure 3b is drawn with simple solid lines for edges, then the 3-D interpretation as a cube is still readily observed. But there is ambiguity about whether the cube is being viewed from above, with its top in the foreground, or from below, with its bottom in the foreground. This ambiguity gives rise to the interesting psychological phenomenon of reversal, in which a prolonged look at the figure commonly involves regular alternations of these two interpretations a few seconds apart. In the two images of Figure 4, we demonstrate the role of the thickness of the beams in suppressing this ambiguity. If the entire image of Figure 4a is scanned for several seconds, it is relatively easy to perceive reversals, despite the contradiction this implies by the image of edge 7 to 3 (or 4 to 3) interposed over edge 5 to 6 (or 2 to 6). It is relatively difficult to perceive these reversals in Figure 4b, presumably due to the more pronounced superposition of these edges using thicker edge beams.

It seems to us that the choice of an appropriate edge beam can be largely configuration and viewpoint independent. Five sided beams have the benefit of showing at least one internal edge from any viewing angle. Bevels of sufficient aspect ratio provide a good resolution of the vertex and allow a large number of beams to be seen to be incident on one vertex.

In our experimenting, we found that much of the time and effort of constructing a satisfying illustration of a complex mesh went into customizing the viewpoint to the configuration. The process we have used has two phases. In the first phase, a global or general viewpoint is determined, and in the second phase, fine tuning of the global view is done. Each viewpoint determines some incidence relations for the 2-D image of the vertices; some of these vertices will lie on the boundary of the image, while the others will lie in internal faces, or on edges, or on other vertex images, in the interior. Choosing a global viewpoint involves deciding which vertices should appear on the boundary of the 2-D images, and ensuring that each other vertex appears in the interior of a face, well separated from other vertices to the extent allowed by the configuration. For example, in Figure 1, vertex $h$ lies in the intersection of the face $dcf$ and face $dce$ of the image. The fine tuning phase then refers to minor adjustments to improve the image, while maintaining these incidence relationships. We have used an interactive graphics display for both phases.

For a complex illustration, fine adjustments of a few degrees of the two viewpoint angles can be worth pursuing, but are tedious to examine and we feel that fine tuning has the potential to be at least partially automated. For a given viewpoint, let us define *an image node* to be either the image of a mesh vertex , or the intersection of two edges. Let us define the *visual circle* of a mesh node to be the largest circle in the 2-D image centered on the node and intersected only by the edges incident on it. The quality of a viewpoint can be quantified by:

i. the minimum radius of the visual circles of the image nodes

ii. the minimum angle that the images of two edges make at an image node.

We have found it useful to compute the gradient of a view quality function such as $F(\theta, \phi) = \min(\alpha \mid \alpha \in A)$ where $A$ is the set of angles referred to in ii. by numerical differentiation with respect to the viewpoint angles $(\theta, \phi)$. We use this gradient as a guide to our next choice of viewpoint during fine tuning. The heuristic motivation is to maximize the minimum angle between the image of two edges, in the sense of a local maximum within the 2-D incidences of a particular global viewpoint. It will be realized that such a maximum occurs when two or more angles take on the value of $\alpha(\min)$ as occurs in Figure 1 in which angles $gbh$ and $bhc$ are equal and are a maximum of the minimal angles for any viewpoint close to the one used in the figure. At such a maximum, $F(\theta, \phi)$ is not differentiable, and its gradient does not approach zero as $(\theta, \phi)$ approach the maximum. In practice, we can often recognize that a viewpoint is close to optimal with regard to $F$ when this gradient changes substantially for small changes in $(\theta, \phi)$ (i.e. changes of a small fraction of a degree). In most of our experimenting with this support for fine tuning, we have used more inclusive performance functions which are less sensitive to discontinuities at their maxima such as $F_{min(k)} = \sum_{i=1}^{k} \alpha_i / i$ where $k$ is a parameter (e.g. $k = 8$) and $\alpha_i$ is the ith smallest angle in the set of angles referred to in ii., above.

We finish this section with some comments on the roles of the secondary mechanisms of the technique, perspective and lighting. We experimented with wide angle perspectives to provide depth cues, and found that its effectiveness is highly configuration and viewpoint dependent. While some striking illustrations can be achieved with a single vertex in the foreground, in general, wide angle effects did not seem predictable enough in advance of trying them, nor did they enhance the comprehension of a complex illustration enough to justify their inclusion in the basic technique. The minor perceptual differences between using the standard perspective and and orthographic one are less apparent when more irregular meshes are being illustrated. We favour the standard perspective mainly for its esthetic effect,

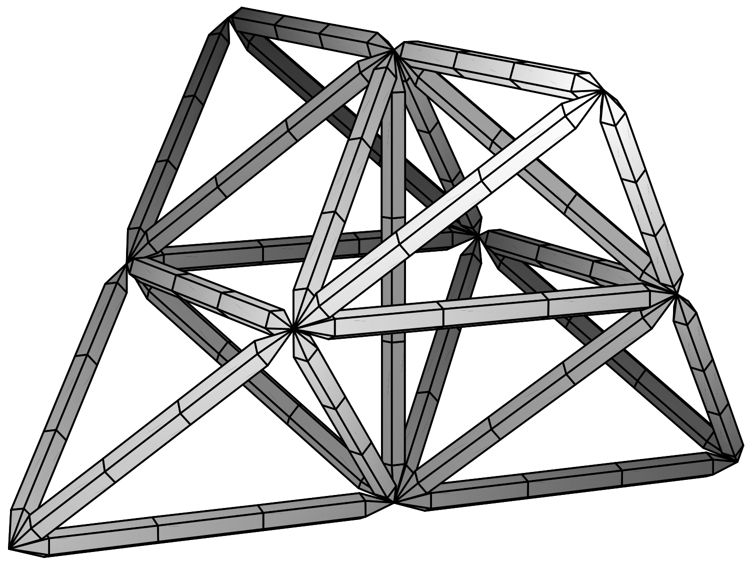

Figure 5: the congruent decomposition of a body centred cubic tetrahedron

although the choice can affect the quality of the best viewpoint , in the sense of the above fine tuning discussion. We experimented with several specular diffuse lighting effects but none seemed be clearly superior to the others, and none provided a clearly identifiable effect of enhancement of the interpretation of an illustration. We have included direct diffuse lighting in the basic technique since it seems most robust (i.e. least dependent on the configuration or other components). We feel that the contribution is almost entirely esthetic, and that illustrations without lighting, as shown in Figure 4b, are usually as effective as shaded ones.

# 4 Some Demonstrations

In this section, we present the basic illustration technique applied to three configurations from the recent literature. The context of these figures has a common theme, i.e., the manner in which some familiar property of two dimensional triangular meshes extends (or does not extend) to tetrahedral meshes. For each case, we will provide a short summary of this context which will provide the interpretation of the figure as a tetrahedral mesh, and direct the reader to the relevant issue of comprehension.

**Demonstration 1 - decomposing the body centred cubic tetrahedron**

It is well-known that the decomposition of any triangle using the midpoints of its sides results in four subtriangles of the same shape as the original. As part of a discussion of tetrahedron based octrees in [FS91], the fact that an analogous decomposition property for tetrahedra only holds for a few special shapes is reviewed. One of these shapes is illustrated in Figure 5, along with its decomposition into 8 subtetrahedra, using the edge midpoints.

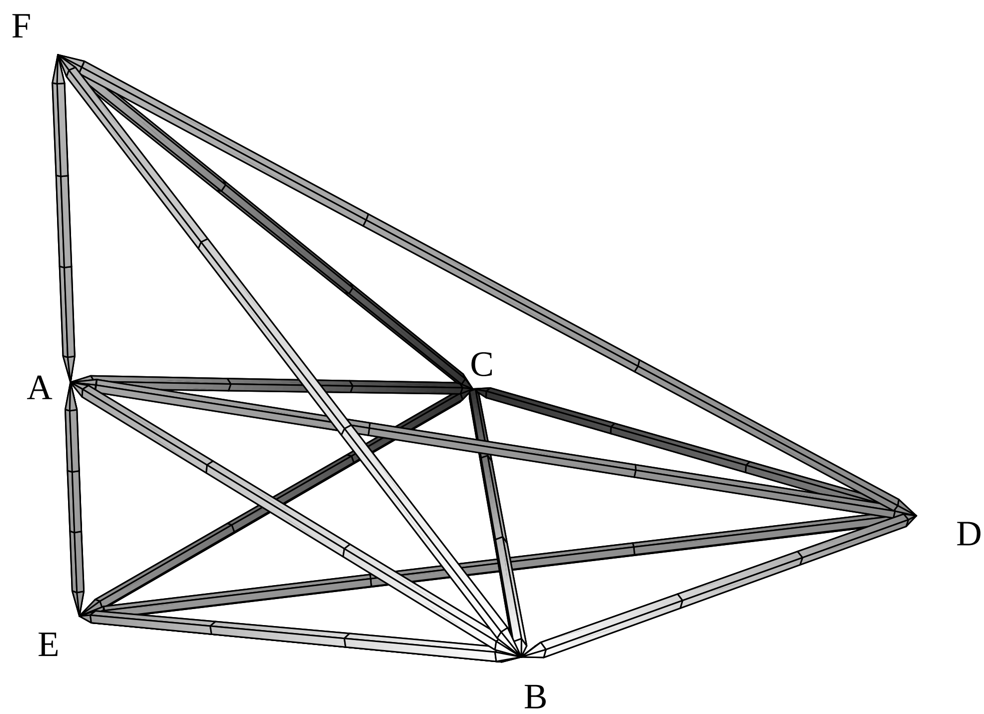


Figure 6: Letniowski's object

This figure has much regularity, so that it is relatively easy to understand the incidence relations of the tetrahedra for its 10 vertices and with 16 external and 8 internal faces. This example perhaps shows that this technique does not illustrate shape information well. It is not easy to recognize that all the tetrahedra of the figure have the same shape.

**Demonstration 2 - Letniowski's object**

In 2-D, there is an equivalence between a monotonicity property of a matrix generated by the finite element method using a triangular mesh and the Delauney property of the triangular mesh being used. The relatively simple configuration of Figure 6 was used in [Let92] as part of a demonstration that this equivalence does not hold in 3-D.

From a comprehension point of view, perhaps the most interesting feature here is the interpretation of the edge, BC. Once a viewer has been directed to regard the configuration as a tetrahedral mesh, there is a strong initial tendency to identify triangle ADE as a tetrahedral face, and the figure as inconsistent because BC passes through it. The resolution is, of course, that ADE is not a tetrahedral face. The illustration is intended to show that there are three tetrahedra incident on BC, containing edges AD, DE, and EA respectively.

This appears to us to be an instance in which the illustration must overcome the psychological phenomenon of seeking the 'simplest' 3-D interpretation of a 2-D image. The role of the textual description in directing the interpretation of this simple figure seems very important to its comprehension.

**Demonstration 3 - a configuration from Barry Joe**

In Figure 7, we show a figure which is more irregular and more difficult to comprehend, although it has only one more vertex than the previous example (7 vertices). A remarkable

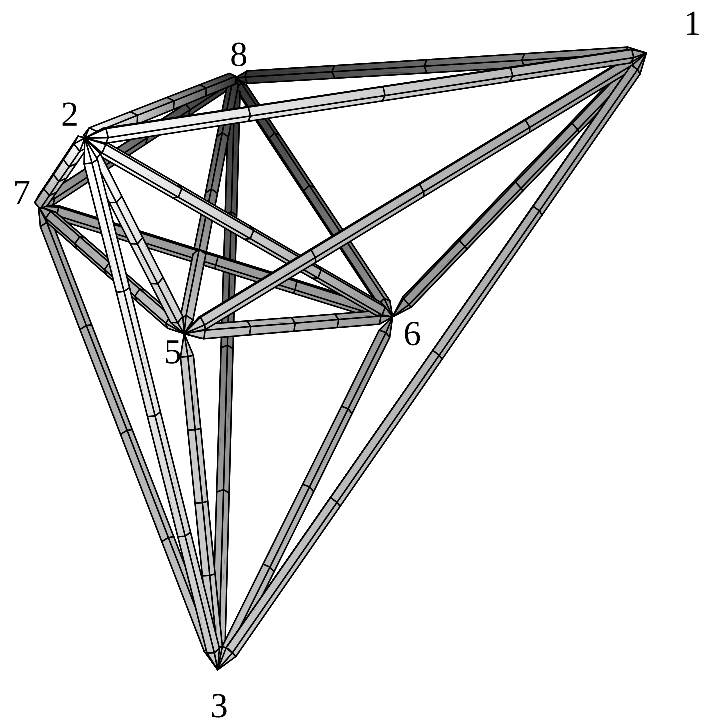


Figure 7: A configuration from Barry Joe

feature of this configuration is that the two tetrahedra incident on each internal face make a non-convex hexahedron.

In two dimensions, it is well-known that the triangulation of a given set of vertices which has the largest minimum angle among all triangulations of these vertices has the following characterization in terms of its edges. For each internal edge, the two triangles incident on it either make a non-convex quadrilateral, or they define a convex quadrilateral and the smallest angle in the current triangulation of this quadrilateral would not be increased by using the triangulation based on its opposite diagonal. The configuration of Figure 7, arises in [Joe89] in connection with demonstrating that a tetrahedral mesh in three dimensions which maximizes the minimum solid angle does not have an analogous characterization in terms of a property of each internal face.

We have also experimented with larger configurations. The usefulness of a single image for supporting understanding of general incidences is probably limited to about 8 to 10 vertices for general meshes. For meshes with a high degree of regularity such as the body centred cubic mesh of demonstration 1, 12 to 15 vertices could be effectively displayed using a full screen (or page) image. An obvious extension would be an investigation of the limitations of two or more static images using this technique. Beyond this, it seems to us that more advanced graphics capability would be necessary to support understanding of 3-D unstructured meshes, probably moving beyond the realm of publication images as currently understood. It is interesting to speculate on the role that a system like the “fish tank” virtual reality of Ware and collaborators ([WAB93] , [WHF93]) could play as an environment for understanding larger unstructured meshes.

# References


[Bob81] D G Bobrow, editor. *Artificial Intelligence: special issue on Computer Vision*, volume 17. North Holland, 1981.

[BT93] H G Barrow and J M Tenenbaum. Retrospective on 'Interpreting line drawings as three-dimensional surfaces'. *Artificial Intelligence*, 59:71–80, 1993.

[C+92] R F Cohen et al. A framework for dynamic graph drawing. In *8th Annual Computational Geometry*, pages 261–270. ACM, 1992.

[FS91] D A Field and W D Smith. Graded tetrahedral finite element meshes. *Intl J for Num Meth in Engg*, 31:413–425, 1991.

[Joe89] B Joe. Three-dimensional triangulations from local transformations. *SISSC*, 10:718–741, 1989.

[Let92] F W Letniowski. Three-dimensional Delaunay triangulations for finite element approximations to a second-order diffusion operator. *SISSC*, 13:765–772, 1992.

[Moo92] D W Moore. Simplical mesh generation with applications. Technical Report 92-1322, Cornell University, Department of Computer Science, 1992.

[Roc75] I Rock. *An Introduction to Perception.* MacMillan, 1975.

[WAB93] C Ware, K Arthur, and K S Booth. Fish tank virtual reality. In *Proc of INTERCHI'93*, pages 37–42. ACM, 1993.

[Wat81] D. F. Watson. Computing the n-dimensional Delaunay tessellation with application to Voronoi polytopes. *The Comp. J.*, 24:167–172, 1981.

[WHF93] C Ware, D Hui, and G Franck. Visualizing object oriented software in three dimensions. In *Proc of CASCON'93*. tba, 1993.